Nanoscale Res Lett (2010) 5:279–285
DOI 10.1007/s11671-009-9476-6

NANO EXPRESS

Preparation of Aligned Ultra-long and Diameter-controlled Silicon Oxide Nanotubes by Plasma Enhanced Chemical Vapor Deposition Using Electrospun PVP Nanofiber Template

Ming Zhou · Jinyuan Zhou · Ruishan Li · Erqing Xie

Received: 14 July 2009 / Accepted: 27 October 2009 / Published online: 19 November 2009

Abstract Well-aligned and suspended polyvinyl pyrrolidone (PVP) nanofibers with 8 mm in length were obtained by electrospinning. Using the aligned suspended PVP nanofibers array as template, aligned ultra-long silicon oxide (SiO*x*) nanotubes with very high aspect ratios have been prepared by plasma-enhanced chemical vapor deposition (PECVD) process. The inner diameter (20–200 nm) and wall thickness (12–90 nm) of tubes were controlled, respectively, by baking the electrospun nanofibers and by coating time without sacrificing the orientation degree and the length of arrays. The micro-PL spectrum of SiO*x* nanotubes shows a strong blue–green emission with a peak at about 514 nm accompanied by two shoulders around 415 and 624 nm. The blue–green emission is caused by the defects in the nanotubes.

Keywords Electrospinning · PECVD · SiO*x* nanotubes · TUFT process

Introduction

Since the discovery of carbon nanotubes in 1991 [1], much effort has been focused on the synthesis of other inorganic tubular nanomaterials, such as MoS_2, BN, TiO_2, VO_X and GaN [2–6]. Nowadays, various inorganic nanotubes have attracted more and more interests in the nanomaterial research [7, 8]. Nanotubes of inorganic materials like silica, which do not have sp^2 bonding that favors tube formation, were generally prepared using porous materials [9, 10] or wire-shaped materials as templates [11]. However, once these templates were removed, the tubes would generally bundle up and become less oriented, even be damaged. Considerable efforts have also been made to prepare aligned silica nanotube arrays to improve their functionality in advanced thin film devices. Fan et al. [12] have developed a process to transformed silicon nanowire arrays into silica nanotube arrays through a thermal oxidation-etching approach. Li et al. [13] have synthesized ultra-long and well-aligned silica nanotubes by the VLS (In as catalyst) mechanism lately. These SiO_2 nanotubes are of special interest because of their potential applications in bioanalysis, bioseparation, optical device and catalysis. Compared with the insulating SiO_2 nanotubes, the silicon monoxide (SiO) nanotubes are predicted to be semiconducting and proposed to have prospective applications in the semiconductor and catalysis industries [14, 15]. Although the studied SiO nanotubes are very thin and only of triangular, tetragonal, pentagonal and hexagonal cross-sections considered, the study suggested a possible route to tailor the electronic structures of silicon oxide (SiO*x*) nanotubes. Meanwhile, the investigation of PL mechanism of SiO*x* nanotubes have important significance because the room temperature PL of porous Si [16, 17] and Si-ion-implanted SiO_2 (SiO_2:Si^+) [18, 19] has stimulated comprehensive studies on light-emitting devices made from Si-based materials. So far, reports of producing SiO*x* nanotubes are still very much lacking [20].

Electrospinning is a simple and highly efficient technique to produce long and extremely fine polymer fiber using an electrostatically repulsive force and an electric field between two electrodes to apply a high voltage to a polymer solution or melt [21, 22]. Meanwhile, different from other nano fiber fabrication processes, electrospinning

M. Zhou · J. Zhou · R. Li · E. Xie (✉)
Key Laboratory For Magnetism and Magnetic Materials of the Ministry of Education, Lanzhou University, 730000 Lanzhou, People's Republic of China
e-mail: xieeq@lzu.edu.cn; zhoum2005@gmail.com

has the ability to form various fiber assemblies [23, 24]. So the approach of using electrospun polymer fibers as templates [25–27] provides great versatility for the design of tubular materials with controlled dimensions. In this work, the preparation of aligned ultra-long and the synthesis of diameter-controlled SiO*x* nanotubes array by plasma-enhanced chemical vapor deposition (PECVD) process using electrospun-suspended polymer fiber array as template are reported. The morphology and chemical compositions of SiO*x* nanotubes were characterized by scanning electron microscope, transmission electron microscope equipped with energy-dispersive X-ray, X-ray photoelectron spectroscopy and micro-Raman. The micro-photoluminescence spectrum was also measured to investigate the luminescence mechanism of SiO*x* nanotubes.

Experimental

Poly(vinyl pyrrolidone) (PVP, 0.18 g, $M_w \approx 1\ 300\ 000$, Sigma–Aldrich) was dissolved in ethanol (3 ml) to form a 7 wt% solution, then loaded to a glass syringe equipped with a stainless steel needle with an inner diameter of 0.34 mm. The needle was connected to a high-voltage supply capable of generating DC voltage up to 60 kV. The voltage for electrospinning was kept at 18 kV. Two pieces of stainless steel stripes with an air gap of 8 mm were placed 18 cm below the tip of the needle [24]. Assisted by electrostatic interactions, the nanofibers were stretched across the gap to form a parallel array. A stainless steel U-shaped frame with a distance of 4 mm between two branches was used to transfer the aligned nanofibers by vertically moving through the gap. The U-shaped frame with suspended nanofiber array span across its two branches was left in dry oven with temperature ranging from 80 to 150°C for 8–10 h to make the PVP template fibers thinner. And then it was transferred to the reaction chamber. The PECVD system is capacitively coupled using a radio frequency (13.56 MHz). After the chamber was pumped down to 3.0×10^{-3} Pa, the pre-treatment of template fibers for surface activation was conducted by the H_2 gas and Ar gas injected into the chamber for 10 min. The applied radio frequency power was 60 W. Then, silane gas with the concentration of 2% flowed into the chamber for the coating. The deposition pressure was 130 Pa. After coating, the aligned core–shell nanofibers were transferred to the surface of silicon wafer by vertically moving silicon wafer through the gap of U-shape frames. Finally, the aligned core–shell nanofibers array was heated at 800°C for 2 h in high-purity argon gas (99.999%) to remove the PVP core, which led to nanotubes array.

The morphology of aligned nanotubes was observed by field emission scanning electron microscope (FE-SEM, Hitachi S-4800) and transmission electron microscope (TEM, JEM-2010, 200 kV). Chemical compositions of the nanotubes were detected using an energy-dispersive spectrometer (EDS) attached to the TEM, X-ray photoelectron spectroscopy (XPS, VG ESCALAB 210) using Mg *K*a radiation and micro-Raman (JY-HR800) with a yttrium aluminum garnet (YAG) laser (532 nm). Furthermore, the micro-photoluminescence (PL) spectrum was measured with a He–Cd laser (325 nm) at room temperature.

Results and Discussion

The selection of the core polymer to be used as the nanofiber template is critical to the process. Polyvinyl pyrrolidone (PVP, $M_w \approx 1{,}300{,}000$) was selected as a suitable template material since it could be processed to fibers with length in the millimeter range, and be stable during coating but degrade under conditions to leave the wall material intact. The equilibrium melting temperature of PVP is 300°C [28], which makes the template fiber thermomechanically stable. Figure 1 shows a SEM image of the aligned PVP nanofibers on a silicon substrate. The enlarged view, shown in the inset, indicates that the average diameter of PVP nanofibers with smooth surface is 200 nm. Figure 2a is a digital image showing the aligned core–shell nanofibers coated by PECVD suspended across the U-shaped frame. The PVP nanofibers were baked from 80 to 150°C for 8–10 h and coated for 6–15 min, but it still kept suspended and tight with a length of 4 mm, indicating that PVP has good thermal and mechanical stability. Figure 2b is optical micrograph of suspended aligned core–shell nanofiber array from one of the samples shown in Fig. 2a. From Figs. 1 and 2, it was clearly that well-aligned and ultra-long PVP nanofibers were obtained by electrospinning over large areas. There are two basic requirements

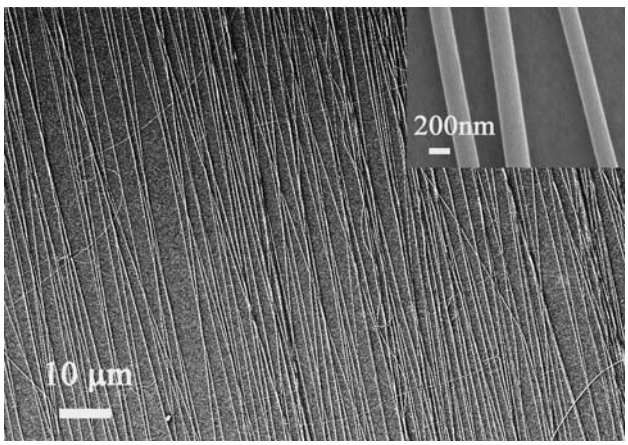

Fig. 1 SEM image of aligned PVP nanofibers. The *inset* is their enlarged view

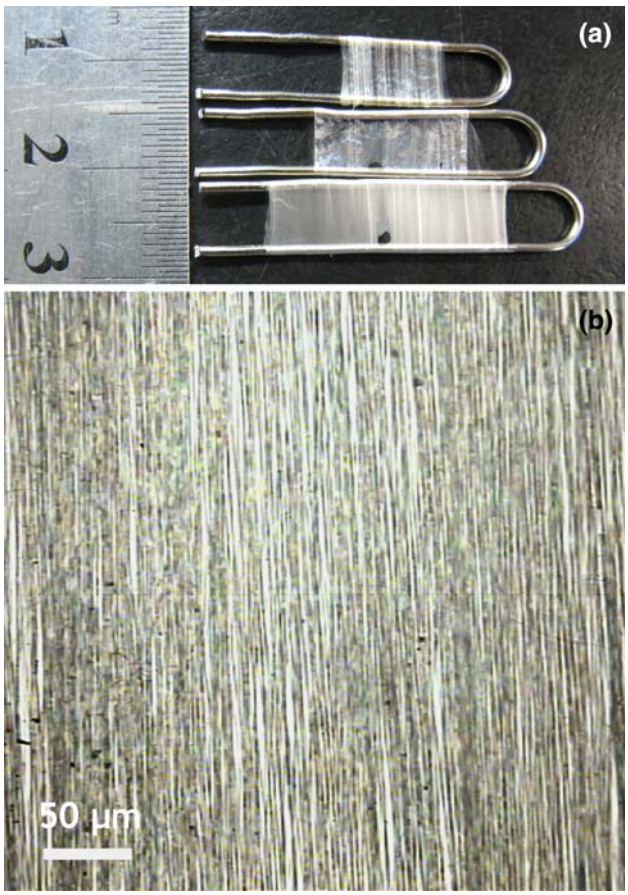

Fig. 2 **a** Digital image and **b** optical micrographs of the aligned core–shell nanofibers suspended over the U-shaped frame

for obtaining highly aligned PVP nanofibers in this process: (i) the jet emerging from the Talylor's cone is stabilized in the effect of electric field; (ii) choosing a suitable gap width and a suitable needle tip-to-target distance. Moreover, the density of the nanofiber array depends on the electrospinning time.

Figure 3a and b show, respectively, low-magnification and high- magnification SEM images of the well-aligned nanotubes, which were obtained after PVP nanofibers were baked at 80°C for 10 h, coated for 10 min and removed by annealing. Most of the nanotubes are straight and have uniform dimensions along their entire lengths. The average outer diameter of the nanotubes is around 170 nm and the surface of nanotubes is smooth. The tubular structures are clearly shown in Fig. 3c. The SEM image of a cross-section of nanotubes reveals that the coating layer did not collapse after PVP template nanofibers were removed by pyrolysis.

Because the nanotubes are aligned and ultra long, it can be physically separated by a simple scratch and put on copper grid without carbon film for TEM observations, which allow us to gain an insight into the prepared tube

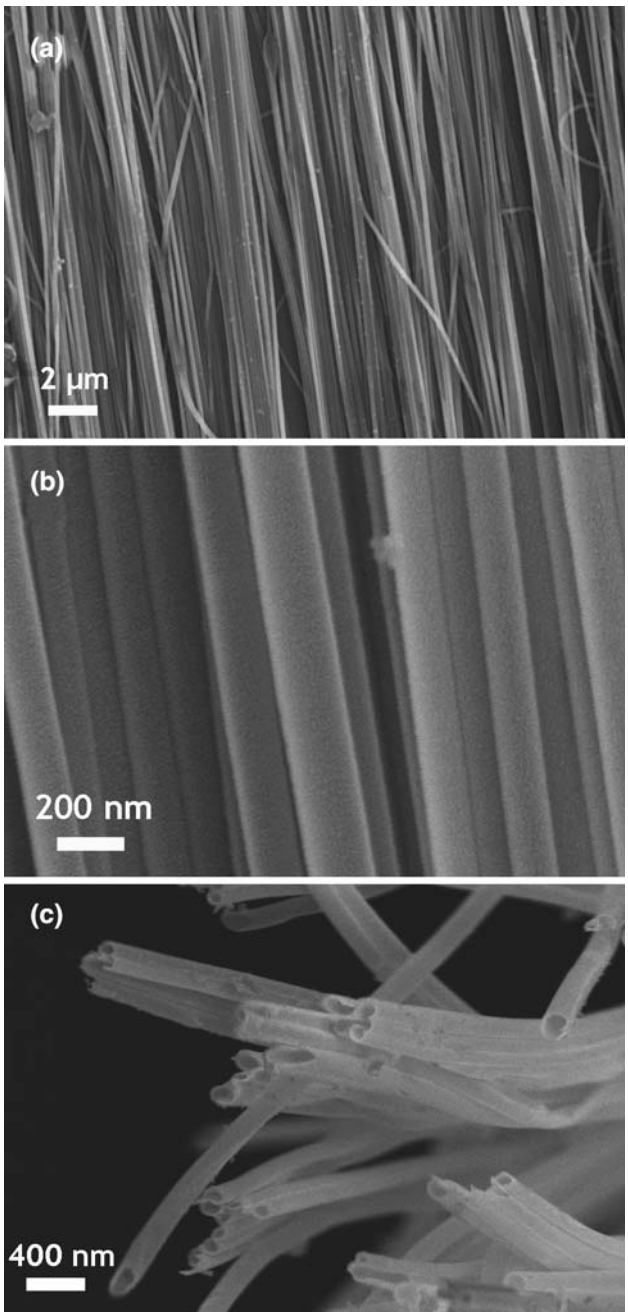

Fig. 3 **a** Low-magnification and **b** high-magnification SEM images of aligned SiO*x* nanotubes. **c** SEM image of a cross-section of SiO*x* nanotubes

structure. Figure 4a and b show, respectively, the TEM images of aligned nanotubes and an individual nanotube prepared in the same condition. There is a distinct boundary between the tube channel and tube wall, and some remainder of PVP pyrolysis is in the tubes channel. The average inner diameter of the nanotubes is approximately 110 nm, which is thinner than the average diameter of electrospun PVP nanofibers. The wall thickness of nanotubes is about 30 nm uniformly corresponding to a

10-min coating time. The highly diffusive ring pattern in the corresponding selected-area electron diffraction (SAED) taken from the individual nanotube reveals these tubular materials are amorphous (inset in Fig. 4b). Figure 4c gives EDX spectrum of the individual nanotube shown in Fig. 4b. Leaving out account Cu from copper TEM grid, the atomic components of the nanotube are $Si_{28.07}$, $O_{34.36}$ and $C_{37.57}$. The result suggests that silicon oxide SiO*x* nanotubes are obtained. The additional carbon peak in the spectrum arises from remainder of PVP pyrolysis [28], which is consistent with the observation in TEM image (Fig. 4a). Considering that the SiO*x* nanotubes are ultra-long and have a smooth tube wall, part of PVP core should be removed through the tube opening, which is also a reasonable answer for question from Liu et al. [27].

Using plastic flake as substrate, the XPS of samples pre and postannealing were obtained. The XPS measurements of the specimen surfaces (~5 nm in depth) indicate that these samples contain Si, O and C. The Si (2p) spectra of samples pre and postannealing are shown in Fig. 5a and b, respectively. According to the random-bonding model, many group analyzed the Si 2p core-level spectra in terms of five chemically shifted components corresponding to

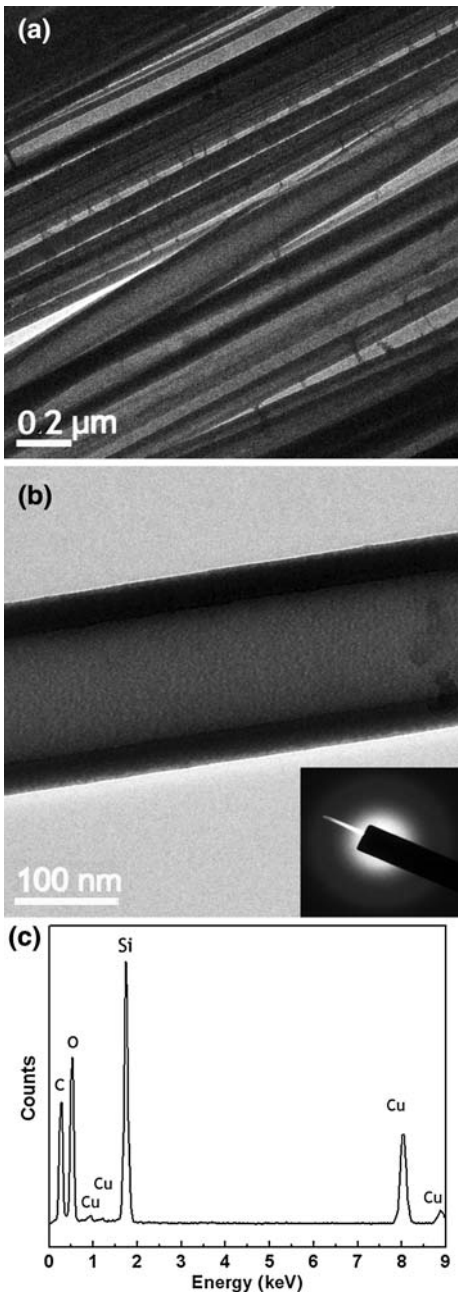

Fig. 4 **a** TEM image of aligned SiO*x* nanotubes. **b** TEM image of an individual SiO*x* nanotube. *Inset* the SAED rings taken from the nanotube. **c** EDX spectrum taken from the SiO*x* nanotube shown in (**b**)

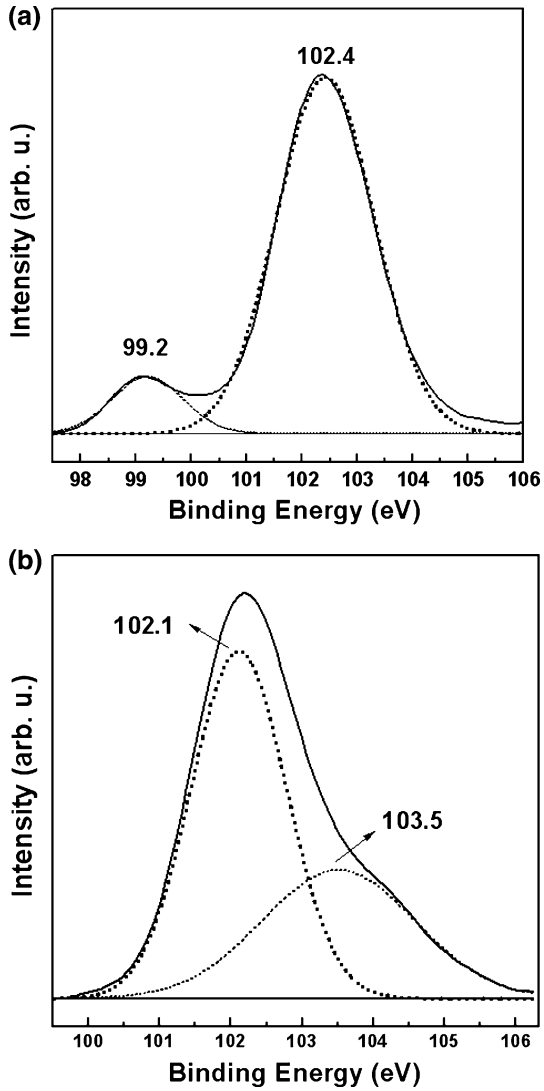

Fig. 5 Fitting analysis of Si 2p core-level spectra of samples **a** pre and **b** postannealing

basic Si bonding units Si–($Si_{4-n}O_n$), with $n = 0, 1, \ldots, 4$ [29–32]. A curve-fitting procedure of the Si 2p core-level line was also adopted in order to identify the inequivalent states of Si. In Fig. 5a, two peaks situated at 99.2 and 102.4 eV are associated with the Si^0 (Si-Si_4) and Si^{3+} (Si-SiO_3), respectively. By contrast, two peaks situated at 102.1 and 103.5 eV are associated with Si^{3+} (Si-SiO_3) and Si^{4+} (Si-O_4), respectively (shown in Fig. 5b). The disappearance of Si^0 (Si-Si_4) and appearance of Si^{4+} (Si-O_4) indicate that the sample is slightly oxidized in the annealing process and thin SiO_2 layers are formed on the surface of SiO*x* nanotubes. This result is unexpected, but it also indicates that the SiO*x* nanotubes can be oxidized completely to SiO_2 by heating the nanotubes in oxygen or air, which is similar to oxidation of SiO*x* film reported by Gonzalez-Elipe et al. [31].

Figure 6 is the micro-Raman spectrum of SiO*x* nanotubes. There is no Si peak in the spectrum, indicating that no silicon particles exist in the tube wall. The D- and G-peaks of graphite at 1,358 and 1,618 cm^{-1} still arise from the remainder of PVP pyrolysis in the tube channel, which is consistent with observation in TEM image and measured results of EDS and XPS.

Generally, the inner diameters of tubes represented the diameters of the polymer template fibers [25]. However, it was found that the average inner diameter (110 nm) (Fig. 4b) of SiO*x* nanotubes was smaller than the average diameter (200 nm) (Fig. 1) of electrospun PVP nanofibers. We deduced that the electrospun PVP nanofibers became fine because of the baking by oven (80°C for 10 h) and plasma etching in the pre-treatment process similar to electron irradiation [33], which led to a smaller inner diameter of nanotubes. To confirm the effect of baking, electrospun PVP template fibers were dried at 150°C for 3 h and at 80°C for 5 h subsequently. TEM images of the sample coated for 6 min are shown in Fig. 7a and b. It can be clearly seen that the average inner diameter of aligned nanotubes is 20 nm, and the wall thickness is about 12 nm, which demonstrates that the diameter of PVP nanofibers or the inner diameter of nanotubes can be controlled by simply baking electrospun PVP fibers. Although the inner diameter of the nanotubes can also be tuned by control of the diameter of template fiber by simply adjusting the physical properties of polymer solution, this usually begeted changes of the solution conductivity further influenced the orientation degree of polymer fibers in spinning process. Moreover, thinner fibers tended to be broken during the spinning process. Therefore, baking offered a simple and effective approach for controlling the diameter of electrospun polymer fibers without sacrificing the orientation degree and the length of arrays. Since the inner diameter of SiO*x* nanotubes decreased, some remainder of PVP pyrolysis was difficult to remove and existed in the tube channel in the form of nanofibers, shown in Fig. 7b. Drying electrospun PVP nanofibers at 80°C for 10 h and prolonging coating time to 15 min increased outer diameter of SiO*x* tube to 300 nm with 90-nm-thick wall, as showing by SEM in Fig 7c and d. The increase of wall thickness would naturally enhance the mechanical properties of the tubes. Because the PVP nanofibers were suspended in the form of alignment in the dissociated gas and had suitable packing density, the thickness of the coated layers was uniform and had a wide varying range. Therefore, the outer diameter of the tubes is governed by the thickness of the tube wall controlled by the CVD conditions (in particular by the coating time), whereas the inner diameter is controlled by the size of the PVP template fibers.

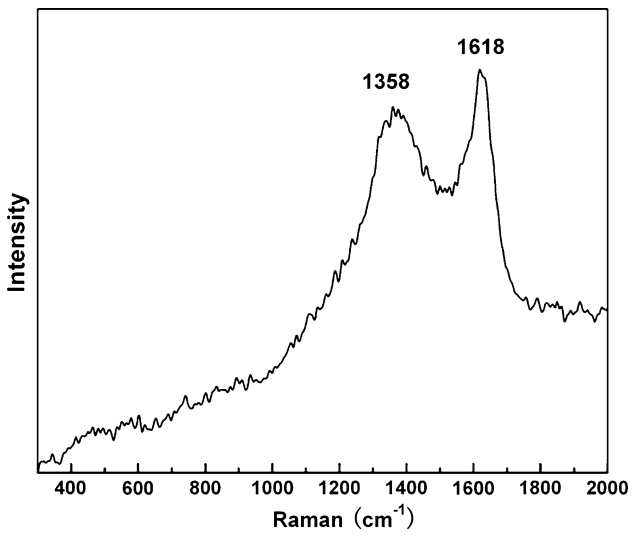

Fig. 6 Raman spectrum of SiO*x* nanotubes

Figure 8 presents the micro-PL spectrum of the SiO*x* nanotubes. Strong blue–green emission from the SiO*x* nanotubes, with at least two peaks at 400–600 nm region was observed. After decomposing with multi-Gaussian function, three luminescent centers at 415, 514 and 624 nm with spectra linewidths of 57, 106 and 157 nm, respectively, are demonstrated. The strongest PL peak at 514 nm is very similar to those obtained by Jiang et al. [20] and Yu et al. [34]. The luminescence at 514 nm reported by Lin et al. [19, 35] has been attributed to the E'_δ defect (a paramagnetic state of Si cluster or a delocalized variant of the E' center). Some observations also suggest that the E'_δ defect is based on the existence of small amorphous Si cluster [36, 37] or its precursor [38] in SiO_2:Si^+ or Si:O^+ materials, which agrees quite well with the measured results of EDS and XPS. Based on the literature data [19, 35, 39], the luminescence at 415 and 620 nm are identified as originating from the weak oxygen bond (WOB) defect

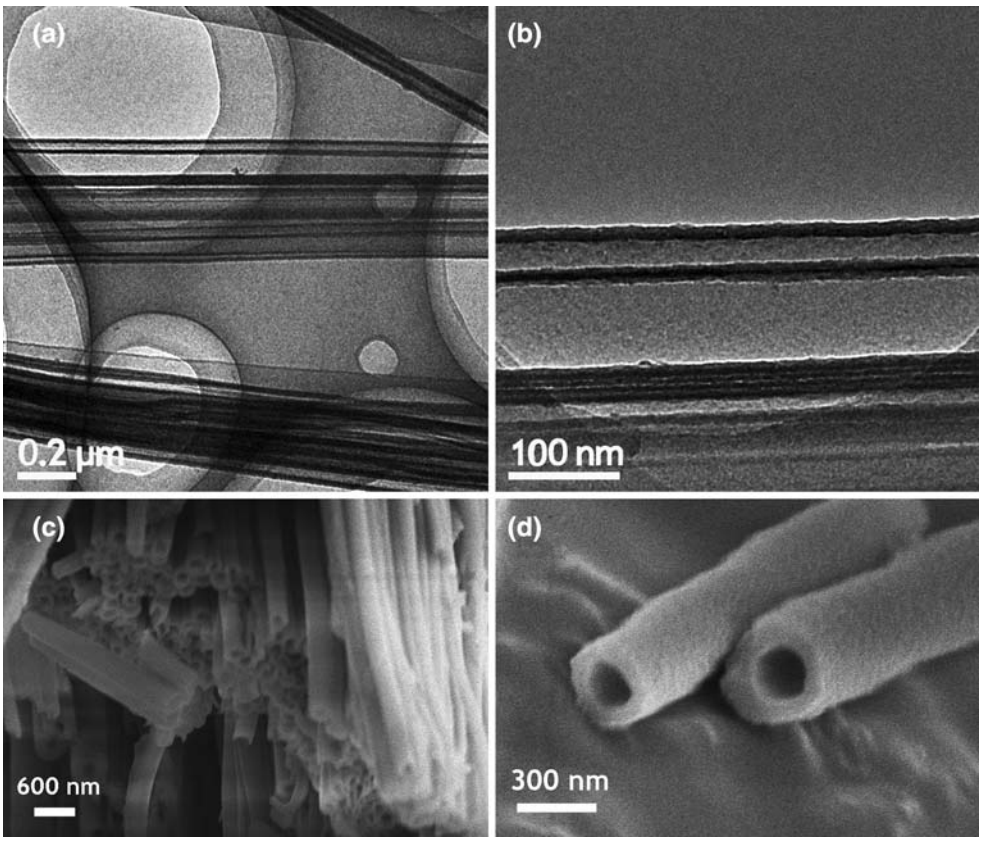

Fig. 7 **a** Low-magnification and **b** high-magnification TEM images of aligned SiO*x* nanotubes with thinner inner diameter. **c** Low-magnification and **d** high-magnification SEM images of a cross-section of SiO*x* nanotubes with thicker tube wall

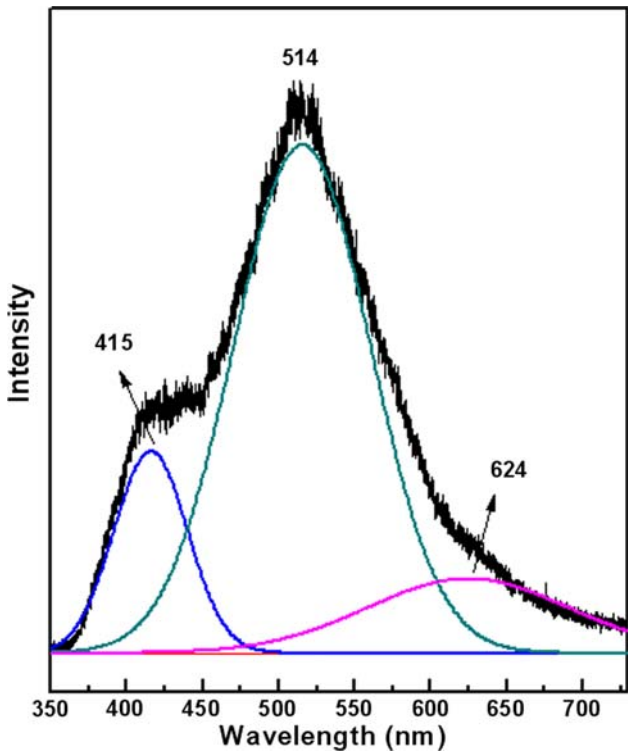

Fig. 8 Micro-PL spectrum of SiO*x* nanotubes

and the nonbridging oxygen hole center (NBOHC) defect, respectively.

Conclusions

In summary, it has been shown that aligned ultra-long SiO*x* nanotubes can be prepared by PECVD system using electrospun aligned PVP template fiber array. The inner diameter and wall thickness of nanotubes were controlled,respectively, by baking the electrospun PVP nanofibers and by coating time without sacrificing the orientation degree and the length of arrays. The PL spectrum of SiO*x* nanotubes shows a blue–green emission with a peak at about 514 nm accompanied by two shoulders around 415 and 624 nm, which is caused by the defects in the nanotubes. Our method shows a great improvement on the basis of tubes by fiber templates (TUFT) process [25] and is a straightforward and easy process for preparing aligned ultra-long SiO*x* nanotubes with very high aspect ratios. These aligned and diameter-controlled SiO*x* nanotubes obtained by us are of great potential for use in nanoscale fluidic bioseparation, sensing, catalysis and nanodevices. Moreover, this method can be used for

preparation of aligned hybrid tubes and nesting structure of nanoparticle/nanofiber/nanotube in tube.

Acknowledgments This work was financially supported by the Program for New Century Excellent Talents in University of China (Grant No: NCET-04-0975).

References

1. S. Iijima, Nature **354**, 56 (1991)
2. Y. Feldman, E. Wasserman, D.J. Srolovitch, R. Tenne, Science **267**, 222 (1995)
3. N.G. Chopra, R.J. Luyken, K. Cherry, V.H. Crespi, M.L. Cohen, S.G. Louie, A. Zettl, Science **269**, 966 (1995)
4. P. Hoyer, Langmuir **12**, 1411 (1996)
5. M.E. Spahr, P. Bitterli, R. Nesper, M. Müller, F. Krumeich, H.U. Nissen, Angew. Chem. Int. Ed. Engl. **37**, 1263 (1998)
6. J. Goldberger, R. He, Y. Zhang, S. Lee, H. Yan, H. Chol, P. Yang, Nature **422**, 599 (2003)
7. X. Sun, Y. Sun, J. Mater. Sci. Technol. **24**, 569 (2008)
8. R. Tenne, Nat. Nanotechnol. **1**, 103 (2006)
9. M. Zhang, E. Ciocan, Y. Bando, K. Wada, L.L. Cheng, P. Pirouz, Appl. Phys. Lett. **80**, 491 (2002)
10. N.I. Kovtyukhova, T.E. Mallouk, T.S. Mayer, Adv. Mater. **15**, 780 (2003)
11. Y.D. Yin, Y. Lu, Y.G. Sun, Y.N. Xia, Nano Lett. **2**, 427 (2002)
12. R. Fan, Y. Wu, D. Li, M. Yue, A. Majumdar, P. Yang, J. Am. Chem. Soc. **125**, 5254 (2003)
13. Y.B. Li, Y. Bando, D. Golberg, Adv. Mater. **16**, 37 (2004)
14. A.K. Singh, V. Kumar, Y. Kawazoe, Phys. Rev. B **72**, 155422 (2005)
15. M.W. Zhao, R.Q. Zhang, Y.Y. Xia, J. Appl. Phys. **102**, 024313 (2007)
16. G.G. Qin, Y.Q. Jia, Solid State Commun. **86**, 559 (1993)
17. G.G. Qin, X.S. Liu, S.Y. Ma, J. Lin, G.Q. Yao, X.Y. Lin, K.X. Lin, Phys. Rev. B **55**, 12876 (1997)
18. H.Z. Song, X.M. Bao, Phys. Rev. B **55**, 6988 (1997)
19. G.R. Lin, C.J. Lin, K.C. Yu, J. Appl. Phys. **96**, 3025 (2004)
20. Z. Jiang, T. Xie, X.Y. Yuan, B.Y. Geng, G.S. Wu, G.Z. Wang, G.W. Meng, L.D. Zhang, Appl. Phys. A **81**, 477 (2005)
21. Y. Dzenis, Science **304**, 1917 (2004)
22. D. Li, Y. Xia, Adv. Mater. **16**, 1151 (2004)
23. W.E. Teo, S. Ramakrishna, Nanotechnology **17**, 89 (2006)
24. D. Li, Y. Wang, Y. Xia, Nano Lett. **3**, 1167 (2003)
25. M. Bognitzki, H. Hou, M. Ishaque, T. Frese, M. Hellwig, C. Schwarte, A. Schaper, J.H. Wendorff, A. Greiner, Adv. Mater. **12**, 637 (2000)
26. R.A. Caruso, J.H. Schattka, A. Greiner, Adv. Mater. **13**, 1577 (2001)
27. W. Liu, M. Graham, E.A. Evans, D.H. Reneker, J. Mater. Res. **17**, 3206 (2002)
28. H. Schmiers, J. Friebel, P. Streubel, R. Hesse, R. Kopsel, Carbon **37**, 1965 (1999)
29. F.G. Bell, L. Ley, Phys. Rev. B **37**, 8383 (1988)
30. T.P. Nguyen, S. Lefrant, J. Phys.: Condens. Matter **1**, 5197 (1989)
31. A. Barranco, F. Yubero, J.P. Espinos, J.P. Holgado, A. Caballero, A.R. Gonzalez-Elipe, J.A. Mejias, Vacuum **67**, 491 (2002)
32. S.M.A. Durrani, M.F. Al-Kuhaili, E.E. Khawaja, J. Phys.: Condens. Matter **15**, 8123 (2003)
33. H.G. Duan, E.Q. Xie, L. Han, Z. Xu, Adv. Mater. **20**, 3284 (2008)
34. Z.G. Bai, D.P. Yu, J.J. Wang, Y.H. Zou, W. Qian, J.S. Fu, S.Q. Feng, J. Xu, L.P. You, Mater. Sci. Eng. B. **72**, 117 (2000)
35. G.R. Lin, C.J. Lin, C.K. Lin, L.J. Chou, Y.L. Chueh, J. Appl. Phys. **97**, 094306 (2005)
36. P. Mutti, G. Ghislotti, S. Bertoni, L. Bonoldi, G.F. Cerofolini, L. Meda, E. Grilli, M. Guzzi, Appl. Phys. Lett. **66**, 851 (1995)
37. H. Takagi, H. Owada, Y. Yamazaki, A. Ishizaki, T. Nakagiri, Appl. Phys. Lett. **56**, 2379 (1990)
38. L.T. Canham, Appl. Phys. Lett. **57**, 1046 (1990)
39. J.C. Cheang-Wong, A. Oliver, J. Roiz, J.M. Hernandez, L. Rodrigues-Fernandez, J.G. Morales, A. Crespo-Sosa, Nucl. Instrum. Methods Phys. Res. B **175–177**, 490 (2001)